"Applications of time-domain metrology to the automation of broadband microwave measurements," *IEEE Trans. Microwave Theory Tech. (Special Issue on Automated Microwave Measurements)*, vol. MTT-20, pp. 3–9, Jan. 1972.
[3] H. M. Cronson and G. F. Ross, "Current status of time-domain metrology in material and distributed network research," *IEEE Trans. Instrum. Meas. (1972 Conf. on Precision Electromagnetic Measurements)*, vol. IM-21, pp. 495–500, Nov. 1972.
[4] H. M. Cronson, P. G. Mitchell, and J. L. Allen, "Time domain metrology study," U. S. Army Missile Command, Redstone Arsenal, AL, Final Rep.–Phase I, SRRC-CR-72-9, Aug. 1972.
[5] R. A. Pucel, D. J. Massé, and C. P. Hartwig, "Losses in microstrip," *IEEE Trans. Microwave Theory Tech.*, vol. MTT-16, pp. 342–350, June 1968.
[6] H. M. Cronson, P. G. Mitchell, J. L. Allen, H. Strenglein, and R. L. Earle, "Time domain metrology study," U. S. Army Missile Command, Redstone Arsenal, AL, Final Rep.–Phase III, SCRC-CR-74-1, Jan. 1974.

Real-Time Fourier Analysis of Spread Spectrum Signals Using Surface-Wave-Implemented Chirp-Z Transformation

GRAHAM R. NUDD, SENIOR MEMBER, IEEE, AND OBERDAN W. OTTO, MEMBER, IEEE

***Abstract*—In many communication and radar applications it is desirable to determine the spectral content of signals in real time. A technique employing dispersive surface acoustic wave devices to implement the chirp-Z transform is described. The experimental results obtained for a number of commonly used signals, including the maximal-length pseudonoise sequences, are shown, and the agreement with theoretical prediction is discussed.**

INTRODUCTION

In many electronic systems a knowledge of the spectral content of received signals in real time provides an invaluable tool which allows the detection process to be rapidly optimized. Correlation receivers, matched filter detection schemes, and systems exhibiting high Doppler shifts are specific examples.

The advent of fast-Fourier-transform techniques has greatly speeded the spectral analysis in recent times, reducing the number of required operations for an N-point transform from N^2 to $N \log_2 N$. However, the cost and power requirements of high-speed digital circuitry has limited its applications in those instances where high speed and low cost are more important than high accuracy. The chirp-Z transformation provides a technique which can be inexpensively implemented using surface acoustic wave devices. In addition to the larger bandwidths, hence higher processing rates available in surface wave devices, the number of operations required for an N-point transform in a chirp-Z transversal filter implementation is N.

Implementation of the chirp-Z algorithm on surface wave devices has been demonstrated with Nyquist rate sampling on a periodically tapped delay line [1] and with continuous sampling in linear FM filters [2], [3]. The implementation utilized here is of the continuous sampling type.

CONCEPT OF TECHNIQUE

A number of authors have pointed out that the Fourier transformation can be expressed in the form of a convolution [4]–[6]. Mertz observed [4] that the operation of multiplication by a chirp prior to Fresnel transformation (convolution with a chirp), and postmultiplication by a chirp corresponds to Fourier transformation. A Fourier transform performed in this manner is referred to as a chirp-Z transform [5]–[6].

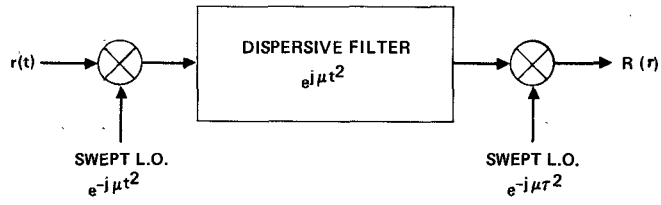

Fig. 1. Schematic of chirp-Z transform.

A linear FM filter of chirp rate μ provides the Fresnel transform $S(\tau)$ of the input $s(t)$

$$S(\tau) = \int dt\, s(t) \exp\left[j\mu(t-\tau)^2 \right]. \tag{1}$$

If the input to the filter $s(t)$ is the signal $r(t)$ multiplied by a chirp

$$s(t) = r(t) \exp\left[-j\mu t^2 \right] \tag{2}$$

and the filter output is also multiplied by a chirp

$$R(\tau) = S(\tau) \exp\left[-j\mu \tau^2 \right] \tag{3}$$

then the final output $R(\tau)$ is the Fourier transform of the input $r(t)$

$$R(\tau) = \int dt\, r(t) \exp\left[-j(2\mu\tau)t \right]. \tag{4}$$

The transformed function $R(\tau)$ appears in real time with the transform frequency proportional to time, the chirp rate μ being the proportionality constant. The chirp-Z implementation of the Fourier transform is illustrated diagramatically in Fig. 1.

EXPERIMENTAL IMPLEMENTATION

In the implementation discussed here, the final mixer stage was not included. This is because the output was displayed in video form and the phase of the carrier was not important. However, if further processing is required before detection, the final de-chirp stage may be required.

Dispersive surface acoustic wave devices were used both for generation of the swept local oscillator signal and for the convolution filter. The devices used had relatively modest time–bandwidth products of 40 with approximately 8-μs dispersion and 5-MHz bandwidth centered at 30 MHz.[1] The input to the first mixer was derived from either a function generator or a programmable data generator with bit rates up to 2 Mbit/s.

The output for a test signal of a single sinusoid of 1 MHz is shown in Fig. 2(a) together with the resulting transform. The transform can be seen to consist of 2 components at frequencies corresponding to ± 2 MHz.

The scanned bandwidth is limited by the filter bandwidth and the number of resolution cells within this is equal to the filter time–bandwidth product. Hence the maximum attainable frequency resolution (f_R) is given by

$$f_R = \frac{\mathrm{B}}{\mathrm{B} \times \tau} = \frac{1}{\tau} = 125\ \mathrm{kHz}.$$

In Fig. 2(b), the results for the same sinusoid with a dc bias are shown, and the corresponding zero frequency component can be seen in the transform. Distortion of the sinusoid is also evident, resulting in second-harmonic spectral components.

Manuscript received May 8, 1975; revised July 24, 1975.
The authors are with the Hughes Research Laboratories, Malibu, CA 90265.

[1] The dispersive delay lines used in this work were designed by the Ground Systems Group, Hughes Aircraft Company, Fullerton, CA.

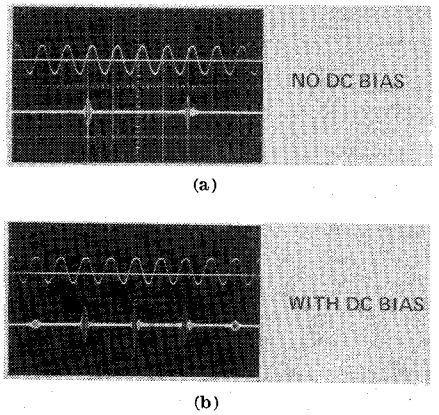

Fig. 2. Transform of a 2-MHz sinusoid. (a) Input signal (scale 0.5 μs/div) and its chirp-Z transform (scale 1 MHz/div). (b) Input signal with dc bias and its chirp-Z transform.

EXPERIMENTAL RESULTS

Of particular importance in modern signaling is the use of waveforms which can be processed at the receiver to enhance their detectability and provide detection gain. The usual procedure in such systems is to encode each data element into a symbol from an *a priori* established alphabet. The transmitted waveforms usually take more complex forms than the baseband data, but since each symbol is one of a set of predetermined waveforms, correlation can be performed at the receiver to enhance the probability of detection. Some penalty has to be paid for the resulting reduced error rates and it is usual to trade bandwidth for detectability.

The optimum waveforms for this type of signaling possess wide bandwidths and good correlation properties such as the Barker sequences [7] and the maximal-length pseudonoise sequences [8]. These formats have many advantageous properties and have found widespread use due to their ease of generation and detection. Recently, surface acoustic wave matched filters [9] have been widely used to detect such sequences. Prior to this, shift registers found wide-spread application for low-bandwidth operation. In either case, however, the number of bits and the bit rate must be known accurately before detection can be achieved. The chirp-Z transform can rapidly determine both of these quantities.

The form of the 13-bit Barker sequence is shown in Fig. 3 together with its experimentally derived chirp-Z transform and its calculated spectrum. The bit rate for this sequence was 3 Mbit/s, and the transform is displayed on a scale of 1 MHz/div. Agreement between experiment and theory is good, and the resolution obtained in frequency is greater than 0.2 MHz. The spectrum, as expected, consists of a number of frequency components spaced at intervals equivalent to the sequence duration; all the energy is nominally contained within a bandwidth $2/T_b$, where T_b is the bit rate. Hence, by observing the frequency difference between adjacent components and counting the number of components to the first null, both the bit rate and sequence length can be determined.

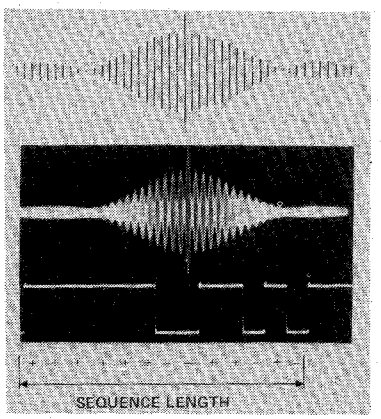

Fig. 3. Transform of 13-bit Barker sequence: calculated transform, experimental transform, time waveform (scales as in Fig. 2).

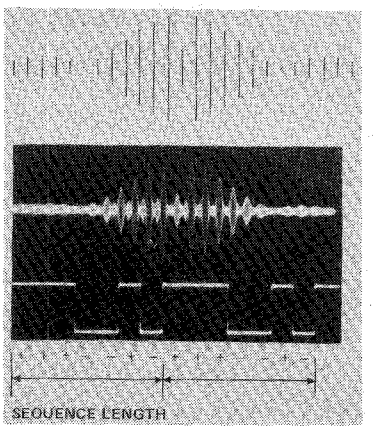

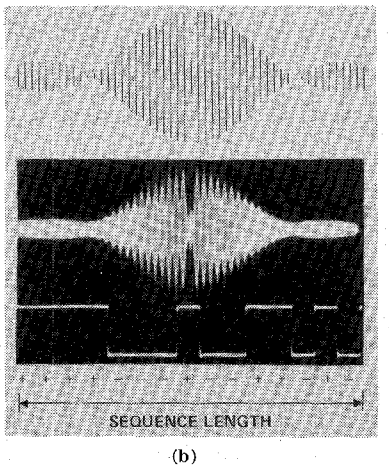

Fig. 4. Transform of pseudonoise sequences. (a) 7-bit P-N sequence: calculated transform, experimental transform, time waveform. (b) 15-bit P-N sequence: calculated transform, experimental transform, time waveform (scales as in Fig. 2).

The maximal-length pseudonoise sequences are not theoretically limited in length and exist in lengths of $2^N - 1$ for all integer N's. The form of the 7-bit and 15-bit sequences and their chirp-Z transforms, and calculated spectra are shown in Fig. 4. Again the energy is concentrated at intervals of the sequence frequency $[(2^N - 1)T_b]^{-1}$ and the nominal bandwidth is equal to the bit rate.

CONCLUSIONS

Good agreement has been obtained between the experimental results and the calculated spectra. The technique can be used as a rapid means of distinguishing different sequences. No attempt was made in this work to increase the resolution by decreasing the adjacent sidelobes and therefore some interference signals can be seen in the results. However, it is anticipated that the commonly used weighting functions such as Hamming [10] can be used to reduce these signals to the order of 40 dB. The resolution obtained is limited by the dispersion in the filter (8 μs), and the code length is determined by the time–bandwidth product (40). The present state of the art indicates that signals with bandwidths in excess of 500 MHz and code lengths of up to 10 000 bit might be processed with acoustic devices [11], [12].

ACKNOWLEDGMENT

The authors wish to thank R. D. Weglein for his active interest during the course of this work.

REFERENCES

[1] J. M. Alsup, R. W. Means, and A. J. Whitehouse, "Real-time discrete Fourier transforms using surface wave acoustic devices," in *Proc. Inst. Elec. Eng. Specialist Conf. Component Performance and System Application of Surface Acoustic Wave Devices* (Aviemore, Scotland, Sept. 1973), pp. 278–285.

[2] O. W. Otto, "Real-time Fourier transform with a surface-wave convolver," *Electron. Lett.*, vol. 8, pp. 623–624, 1972.

[3] J. B. Harrington, "VHF/UHF compressive receiver study," Rome Air Development Center, Final Rep., Contract F30602-71-C-0347, Nov. 1972.

[4] L. Mertz, *Transformations in Optics*. New York: Wiley, 1965, p. 94.

[5] L. I. Bluestein, "A linear filtering approach to the computation of the discrete Fourier transform," *NEREM Rec.*, pp. 218–219, Nov. 1968.

[6] L. R. Rabiner, R. W. Schaffer, and C. M. Rader, "The chirp-*Z* transform algorithm and its application," *Bell Syst. Tech. J.*, vol. 48, pp. 1249–1292, Jan.–June 1969.

[7] R. H. Barker, "Group synchronizing of binary digital systems," in *Communication Theory*, W. Jackson, Ed. New York: Academic, 1953, pp. 273–287.

[8] M. F. Easterling, "Modulation by pseudo-random sequences," in *Digital Communications*, W. L. Everitt, Ed. Englewood Cliffs, NJ: Prentice-Hall, 1964, pp. 65–84.

[9] B. J. Darby, P. M. Grand, J. A. Collins, and I. M. Crosby, "Performance of aposiodic spread spectrum incorporating surface acoustic wave analog matched filters," in *Proc. Inst. Elec. Eng. Specialist Conf. Component Performance and System Application of Surface Acoustic Wave Devices* (Aviemore, Scotland, Sept. 1973), pp. 278–286.

[10] C. L. Temes, "Sidelobe suppression in range-channel pulse-compression radar," *IRE Trans. Mil. Electron. (Special Issue on Signal Processing Radar)*, vol. MIL-6, pp. 162–169, Apr. 1962.

[11] R. C. Williamson, V. S. Dolat, and H. I. Smith, "L-band reflective array compressor with a compression ratio of 5120," in *Proc. 1973 IEEE Ultrasonics Symp.* (Monterey, CA, 1973), pp. 490–493.

[12] H. M. Gerard, O. W. Otto, and R. D. Weglein, "Development of a broad-band reflective array 10,000:1 pulse compression filter," in *Proc. 1974 IEEE Ultrasonics Symp.* (Milwaukee, WI, 1974), pp. 197–201.

Waveguide Interferometer for Measuring Electric Susceptibility in Gases

G. P. SRIVASTAVA, SENIOR MEMBER, IEEE,
P. C. MATHUR, SENIOR MEMBER, IEEE, AND
ANIL KUMAR, STUDENT MEMBER, IEEE

***Abstract*—A simple, quick, and accurate method employing a magic-T interferometer for the measurement of electric susceptibility in gases is presented in this short paper. The electric susceptibility of five substances in a gaseous state has been measured satisfactorily as a function of pressure at room temperature with the help of this setup.**

INTRODUCTION

The electric susceptibility of gases in the microwave region is usually determined by two techniques. The first technique is based on the measurement of the shift in the resonant frequency of a cavity with the dielectric material kept inside it. This method has been used by Jen [1] and Birnbaum *et al.* [2]. In the second method, the shift in the standing wave is measured with the experimental gas in the waveguide cell. This method has been used by Hershberger [3], Krishnaji [4], and Srivastava [5].

Manuscript received March 26, 1975; revised June 23, 1975.

The authors are with the Department of Physics and Astrophysics, University of Delhi, Delhi-110007, India.

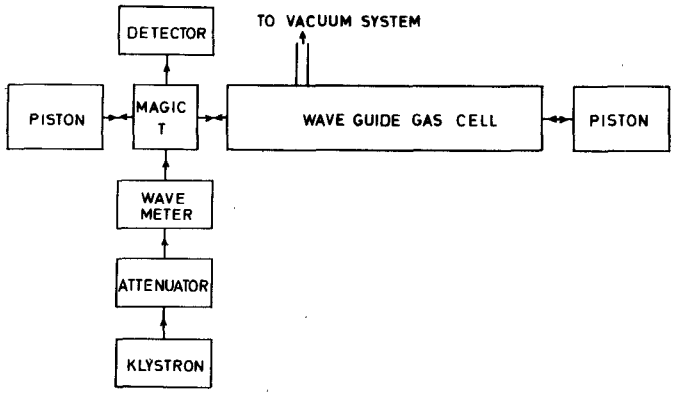

Fig. 1. Block diagram of interferometer setup used.

With the method presented here, a magic T is used to detect the change of phase when the gas is introduced into the cell. From this change of phase, the electric susceptibility can be calculated easily.

Experimental Setup

The block diagram of the interferometer is shown in Fig. 1. The microwave source, the attenuator, and the wavemeter are connected to the *H*-plane arm of Magic T (arm *A*). A 10-ft-long waveguide cell fitted with a mica window shorted at another end is connected to one of arm (*B*) of the magic T. Opposite to arm *B*, a movable short (piston) is connected in arm *C*. The crystal detector with matched load is placed in the *E*-plane arm of the magic T (arm *D*). Adjusting the position of the movable short in arm *C*, the minimum power at the detector arm can be achieved with and without gas in the absorption cell.

If the magic T is not perfect, it can be tuned to a particular frequency at which it works satisfactory. In the setup presented here, the magic T is tuned to a frequency of 9.55 GHz. The plunger used in the arm *C* has a clearance of 0.22 mm from the walls of the waveguide all around; this prevents the leakage of power past it. By means of a micrometer adjustment, the position of the piston could be set up to an accuracy of 0.05 mm. The output power of the crystal detector (IN23B) is fed to a sensitive galvanometer or nanovoltmeter.

THEORY OF THE EXPERIMENT

Let

λ_{fs} free-space wavelength in vacuum;
λ_{vg} guide wavelength in vacuum;
λ_{gg} guide wavelength in dielectric gas;
λ_c cutoff wavelength = $2b$.

Then for the TE_{10} mode in a rectangular waveguide

$$\lambda_{vg} = \lambda_{fs}\left[1 - \left(\frac{\lambda_{fs}}{\lambda_c}\right)^2\right]^{-1/2}$$

and $\epsilon = 1 + \delta$, where δ is the electric susceptibility of gases, the

$$\lambda_{gg} = \lambda_{fs}\left[1 + \delta - \left(\frac{\lambda_{fs}}{\lambda_c}\right)^2\right]^{-1/2}.$$

Therefore